Study of Regular and Irregular States in Generic Systems

Gregor Veble, Marko Robnik and Junxian Liu*)

Center for Applied Mathematics and Theoretical Physics
University of Maribor, Krekova 2, SI-2000 Maribor, Slovenia

In this work we semiclassically analyzed the high lying eigenstates of a mixed type Hamiltonian system. For the regular states we employ the Einstein-Brillouin-Keller quantization, while for the chaotic states, following the principle of uniform semiclassical condensation, we obtain a prediction for their wavefunction autocorrelation function.

§1. Introduction

Classical Hamiltonian systems can range from completely integrable ones, such as the Kepler problem and the harmonic oscillator, to fully chaotic systems (e.g. Bunimovich stadium, Sinai billiards). Yet the majority of classical systems fall into neither category but are of the generic, mixed type. The phase space of such systems is split into areas of quasiperiodic motion on phase-space tori like in the integrable systems, and into areas where the motion is chaotic.

The quantum mechanical properties of classically integrable and classically chaotic systems vastly differ in the semiclassical limit $\hbar \to 0$. The Wigner functions (the quantum mechanical analogues of the classical phase space density) of eigenstates of integrable systems are localized on tori in phase space, and the eigenfunctions in configuration space have an ordered structure. On the other hand, the eigenfunctions of fully chaotic/ergodic systems appear random [1),2)] and their Wigner functions uniformly cover the whole energy shell in the phase space.

For the mixed type systems the principle of uniform semiclassical condensation (PUSC, see Refs. 3), 4)) states that the Wigner functions should in this case be localized either on the invariant tori in the regions of regular motion or should uniformly cover the whole chaotic component of the energy shell in the phase space. This means that states are separated into regular and irregular ones.

In this work we are interested in geometrical and statistical properties of both regular and irregular high lying eigenfunctions. For the regular states we employ the Einstein-Brillouin-Keller (EBK) quantization, while for the chaotic states we give an expression for the wavefunction autocorrelation function based on the geometry of the chaotic component in the classical phase space. For more details see Ref. 5) and references therein. Recently we also performed experiments with microwave cavities on the same mixed type system as presented here,[6)] while theoretical work on another mixed type system has been done by Makino et al.[7)]

*) e-mails: gregor.veble@uni-mb.si, robnik@uni-mb.si, jliu@tikva.chem.utoronto.ca

§2. Definitions

Our model system was a billiard obtained by conformally mapping the unit circle with the complex quadratic polynomial, [8),9)]

$$z \to w(z) = z + \lambda z^2,\ w(z) = x + iy. \tag{2·1}$$

We chose $\lambda = 0.15$, where the classical phase space is roughly equally divided into components of regular and chaotic motion. The Poincaré surface of section (SOS) was chosen to lie on the symmetry axis $y = 0$ with coordinate x and the conjugate momentum p_x as the parameters of the surface. The intersection of the main chaotic component of our billiard with the SOS is shown in Fig. 1. The coordinate x is taken relative to the center of the billiard, while p_x is the x-component of the unit momentum vector.

The quantum mechanics of billiards is described by the Helmholtz equation

$$(\Delta + k^2)\psi = 0, \tag{2·2}$$

with the Dirichlet boundary conditions, where $k^2 = 2mE/\hbar^2$. We limited ourselves to the states with even parity with respect to reflection across the symmetry line $y = 0$.

For each state we calculated the smoothed projection of the Wigner function. The Wigner function of a state $\psi(\boldsymbol{q})$ in the general case of N degrees of freedom is defined in the full phase space $(\boldsymbol{q}, \boldsymbol{p})$ as [10)]

$$W(\boldsymbol{q}, \boldsymbol{p}) = \frac{1}{(2\pi\hbar)^N} \int d^N \boldsymbol{X} \exp(-i\boldsymbol{p} \cdot \boldsymbol{X}/\hbar)\psi^\dagger(\boldsymbol{q} - \boldsymbol{X}/2)\psi(\boldsymbol{q} + \boldsymbol{X}/2). \tag{2·3}$$

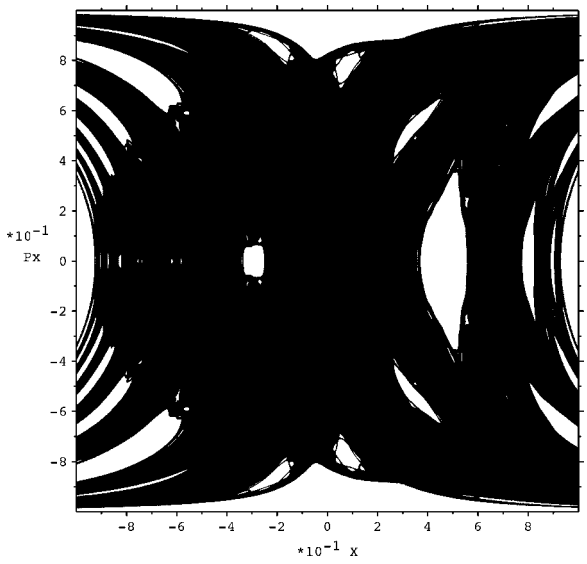

Fig. 1. The SOS section of the main chaotic component of the $\lambda = 0.15$ billiard.

In our case the eigenfunctions $\psi(x, y)$ generate their Wigner transforms $W(x, y, p_x, p_y)$ through (2·3), where $N = 2$. In order to compare the Wigner function of a state of our system with the classical SOS plot we took its value on the symmetry line ($y = 0$) and integrated it over p_y,

$$\rho_{\mathrm{SOS}}(x, p_x) = \int dp_y W(x, y = 0, p_x, p_y). \tag{2·4}$$

The result is

$$\rho_{\mathrm{SOS}}(x, p_x) = \frac{1}{2\pi\hbar} \int dX \exp(-ip_x X/\hbar)\psi^{\dagger}(x - X/2, y = 0)\psi(x + X/2, y = 0). \tag{2·5}$$

Here we see the reason for considering the even parity states only, because $\psi(x, y = 0)$ is exactly zero for odd states, and therefore a different approach must be used to analyze them.

The catalogue of states studied here consists of 100 consecutive states starting at the consecutive index of about $2.5 \cdot 10^6$. These states were obtained by the scaling method first introduced by Vergini and Saraceno,[11] that enables us to find a few states in the neighbourhood of a chosen wavenumber k. As this is a diagonalizational method no levels were missed. Almost each level in our small catalogue can be clearly identified as regular or irregular, an idea proposed already by Percival.[12]

§3. Analysis of states

In a mixed system the phase space is divided into chaotic and regular components. Our work was guided by the principle of uniform semiclassical condensation (PUSC, see Robnik 1998), stating that when $\hbar$ tends to 0 the Wigner function of any eigenstate uniformly condenses on an invariant object in phase space. This can be either a torus in the regular region or a whole chaotic component. Each state could thus be labeled as either regular or irregular (chaotic) in the semiclassical limit. By looking at the catalogue of states at high (and to some extent even at low) energies, one can see that this can indeed be done, though there is still the localization phenomenon present due to the still insufficiently low value of the effective Planck's constant.

3.1. *Regular states*

We start the analysis by considering the regular states. These are the states that can be attributed to quantized tori within the regular regions. For these states we tried to employ the EBK torus quantization. We construct a wavefunction on the torus as a sum of contributions

$$\psi_j(\boldsymbol{q}) = A_j(\boldsymbol{q}) \exp\left(i\left[\frac{1}{\hbar} S_j^{cl}\boldsymbol{q}) + \phi_j\right]\right) \tag{3·1}$$

of different projections j of the torus onto configuration space. S_j is the classical action with respect to some point on the torus and A_j^2 the classical density of trajectories on this projection. The phase of the wavefunction must change by an integer

multiple of 2π when going around any closed contour of the torus. This gives us the quantization conditions

$$I_i = \frac{1}{2\pi} \oint_{\gamma_i} \boldsymbol{p} \cdot d\boldsymbol{q} = \hbar(n_i + \beta_i/4), \tag{3·2}$$

where γ_i are the irreducible closed contours on the torus and n_i the torus quantum numbers. The integers β_i are Maslov's corrections and arise due to the changes of phase ϕ_j at the singularities of projection of the torus onto configuration space. At each caustic encountered along the contour γ_i the wavefunction acquires a negative

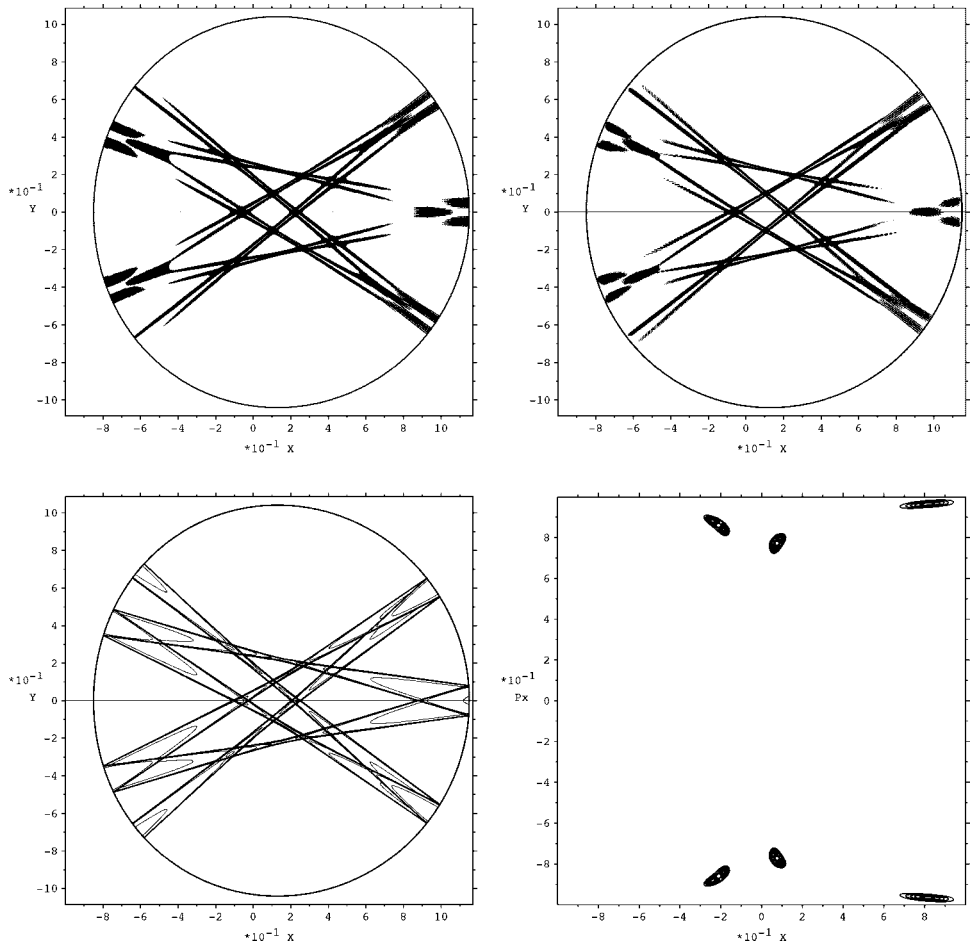

Fig. 2. The probability density for a regular state with $k^2 = 20421387.1741$ (top left), its semi-classical approximation with $k_{sc}^2 = 20421385.96$ (top right), with the quantum numbers on the torus being $n_1 = 8648$ and $n_2 = 1$ (16 equally spaced contours from 0 to the maximum value in both cases). In the bottom row we show the classical density with 20 contours from 0 to the maximum of the appropriate torus (left) and the smoothed projection of the exact Wigner function (right), with ten contours from 0 to the maximum value.

phase shift of $\pi/2$, and shifts by π when reflected from a hard wall.*) From this consideration it follows that β_i counts the number of caustics plus twice the number of hard walls encountered along the contour.

The task of finding the semiclassical EBK wavefunctions can be divided into two parts. The first one is finding the torus with the desired quantum numbers n_i, the second one being the construction of its appropriate wavefunction in configuration space. This is not very straightforward since we do not know the transformation to the torus action-angle variables but can only deal with the numerically calculated orbits. For more details on this procedure see Ref. 5).

We show an example of a regular state in Fig. 2. We present the exact numerical quantum probability density (top left), the probability density of its semiclassical approximation (top right), the classical density of trajectories on the appropriate torus (bottom left) and the smoothed projection of the exact Wigner function (bottom right). The semiclassical wavefunctions shown are remarkable as they possess all of the features of their exact counterparts that are larger than the appropriate wavelength. Note that for each torus there are two characteristic wavelengths since there are two quantum numbers associated with it. As it happens in our case, the two wavelengths can be of different orders of magnitude.

3.2. *Irregular states*

While for the regular states it was quite straightforward to find their semiclassical approximations, the nature of irregular states is very much different. These states are very sensitive to small perturbations of the system, so in any physical system the individual features of the states are lost when the effective Planck's constant tends to 0. The features that are insensitive to small perturbations are, however, the statistical properties of spectra and eigenstates.

One measure of statistical properties of the wavefunctions is the wavefunction autocorrelation function,

$$C(\boldsymbol{q},\boldsymbol{x}) = \frac{\langle \psi^\dagger(\boldsymbol{q}'-\boldsymbol{x}/2)\psi(\boldsymbol{q}'+\boldsymbol{x}/2)\rangle_{\boldsymbol{q}'\in\epsilon(\boldsymbol{q})}}{\langle \psi^\dagger(\boldsymbol{q}')\psi(\boldsymbol{q}')\rangle_{\boldsymbol{q}'\in\epsilon(\boldsymbol{q})}}. \tag{3·3}$$

The area of averaging $\epsilon(\boldsymbol{q})$ close to the point $\boldsymbol{q}$ should be taken such that its linear size is many wavelengths across, however small enough that the local properties of classical mechanics within it are largely uniform.

If one takes the Fourier transform of the Wigner function (2·3), it is easy to show that

$$\int W(\boldsymbol{q},\boldsymbol{p})\exp(i\boldsymbol{p}\cdot\boldsymbol{x}/\hbar)d^N\boldsymbol{p} = \psi^\dagger(\boldsymbol{q}-\boldsymbol{x}/2)\psi(\boldsymbol{q}+\boldsymbol{x}/2). \tag{3·4}$$

By knowing the Wigner function of an eigenstate, it is then possible to use this result to calculate its autocorrelation function.

According to the principle of uniform semiclassical condensation, the Wigner function of any chaotic state should uniformly condense on the whole chaotic com-

*) If the contour passes the singularity in the contrary direction to that of the Hamiltonian flow on the torus, the phase shifts are of the opposite sign.

ponent when the effective $\hbar$ tends to 0. Let us limit ourselves only to the cases of the Hamiltonians with an isotropic dependence upon $\boldsymbol{p}$. We can write the semiclassical Wigner function as

$$W_{\mathcal{D}_i}(\boldsymbol{q},\boldsymbol{p}) = \alpha\delta(E - H(\boldsymbol{q},p))\chi_{\mathcal{D}_i}(\boldsymbol{q},\boldsymbol{p}), \tag{3·5}$$

where $\chi_{\mathcal{D}_i}$ denotes the characteristic function of the chaotic component and α is the normalization constant.

If we write the characteristic function in two degrees of freedom as a Fourier series of the polar angle ϕ_p of the momentum vector (since the absolute value of $\boldsymbol{p}$ is constant at a given energy and point $\boldsymbol{q}$),

$$\chi_{\mathcal{D}_i}(\boldsymbol{q},\boldsymbol{p}) = \sum_{m=-\infty}^{\infty} \kappa_m^{\mathcal{D}_i}(\boldsymbol{q}) \exp(im\phi_p), \tag{3·6}$$

it is quite straightforward to show by using the above expressions and the integral

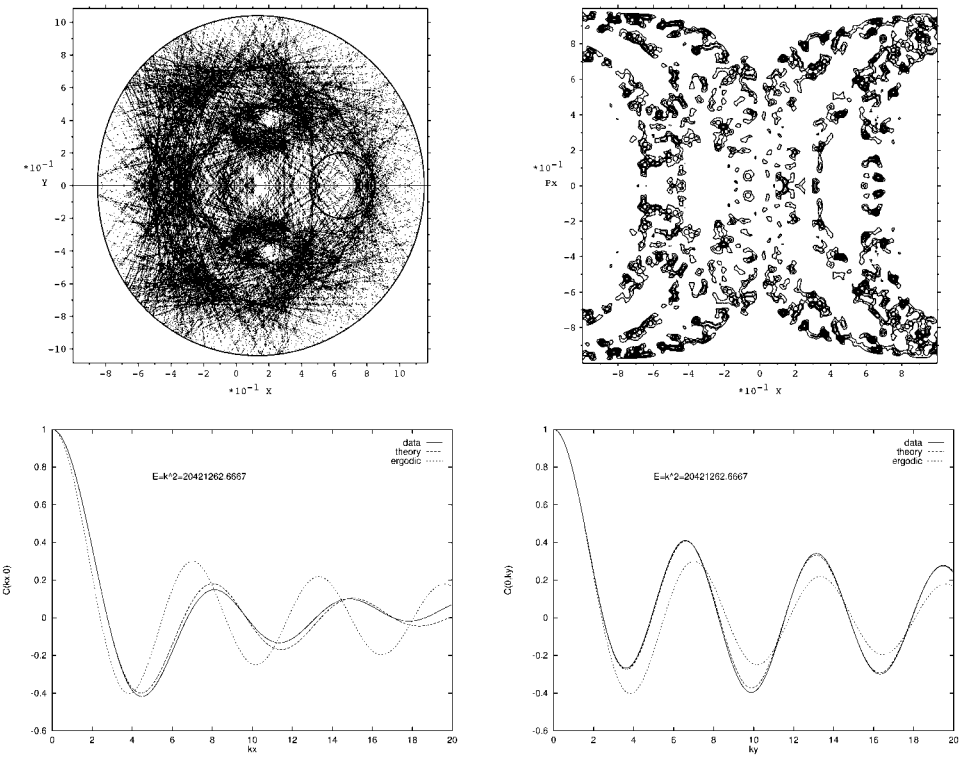

Fig. 3. In the top row we show the probability density for the chaotic state with $k^2 = 20421262.6667$ (left, 8 contours), the circle denoting the region of averaging, with the smoothed projection of its Wigner function (right, 10 contours). In the bottom row we plot the wavefunction autocorrelation function (averaged as explained in text) in the x (left) and y (right) directions (full), compared to the semiclassical prediction (dashed) and the fully ergodic prediction (dotted).

representations of the Bessel functions that

$$C_{\mathcal{D}_i}(\boldsymbol{q},\boldsymbol{x}) = \frac{\langle \sum_{m=-\infty}^{\infty} \kappa_m^{\mathcal{D}_i}(\boldsymbol{q}') i^m J_m(p(\boldsymbol{q}')r/\hbar)\exp(im\phi_x)\rangle_{\boldsymbol{q}'\in\epsilon(\boldsymbol{q})}}{\langle \kappa_0^{\mathcal{D}_i}(\boldsymbol{q}')\rangle_{\boldsymbol{q}'\in\epsilon(\boldsymbol{q})}}, \qquad (3\cdot7)$$

where ϕ_x is the polar angle of the vector $\boldsymbol{x}$.

We compare the autocorrelation function of a chaotic state with the semiclassical prediction (3·7) in Fig. 3. The averaging area $\epsilon(\boldsymbol{q})$ was taken as a circle of radius 0.2 around the point $(x, y) = (0.65, 0)$. It was taken the same for both the semiclassical prediction and for the numerical results. The averaging radius was taken quite large in order to reduce the localization properties of the wavefunctions, which are still apparent at the values of effective $\hbar$ that we were able to obtain. But this radius still has to be taken small enough in order not to completely smooth out the classical dynamics. The agreement with the semiclassical prediction is quite good. It clearly deviates from the Berry's prediction [1)] for fully ergodic systems and tends towards our semiclassical result.

§4. Conclusion

In this work we were able to find semiclassical wavefunctions of the regular eigenstates, while for the chaotic states we gave a prediction for the wavefunction autocorrelation function, both of which match nicely with their exact counterparts. What needs to be studied further is the localization of the chaotic states on only parts of the whole chaotic component when not yet in the strict semiclassical limit, which gives rise to deviations from semiclassical predictions.

Acknowledgements

We thank Dr. Tomaž Prosen for assistance and advice with some computer programs. This work was supported by the Ministry of Science and Technology of the Republic of Slovenia and by the Rector's Fund of the university of Maribor.

References

1) M. V. Berry, J. of Phys. A: Math. Gen. **10** (1977), 2083.
2) A. Voros, *Lecture Notes in Physics* **93** (1979), 326.
3) M. Robnik, *Atomic Spectra and Collisions in External Fields*, ed. K. T. Taylor, M. H. Nayfeh and C. W. Clark (New York: Plenum Press, 1988), p. 251.
4) M. Robnik, Nonlinear Phenomena in Complex Systems **1** (1988), 1.
5) G. Veble, M. Robnik and J. Liu, J. of Phys. A: Math. Gen. **32** (1999), 6423.
6) G. Veble, U. Kuhl, M. Robnik, H.-J. Stöckmann, J. Liu and M. Barth, Prow. Theory. Phys. Suppl. No. 139 (2000), 283.
7) H. Makino, T. Harayama and Y. Aizawa, Phys. Rev. **E59** (1999), 4026.
8) M. Robnik, J. of Phys. A: Math. Gen. **16** (1983), 3971.
9) M. Robnik, J. of Phys. A: Math. Gen. **17** (1984), 1049.
10) M. V. Berry, *Chaotic Behaviour of deterministic Systems (Proc. NATO ASI Les Houches Summer School)*, ed. G. Iooss, R. H. G. Helleman and R. Stora (Elsevier, Amsterdam, 1983), p. 171.
11) E. Vergini and M. Saraceno, Phys. Rev. **E52** (1995), 2204.
12) I. C. Percival, J. of Phys. B: At. Mol. Phys. **6** (1973), L229.